JOURNAL OF MATERIALS SCIENCE 30 (1995) 3612–3618

Transport property and battery discharge characteristic studies on $1-x$(0.75AgI:0.25AgCl):xAl_2O_3 composite electrolyte system

R. C. AGRAWAL*, R. K. GUPTA
Solid State Ionics Research Laboratory, School of Studies in Physics, Pt. Ravishankar Shukla University, Raipur 492 010, India

Various experimental studies on a new fast Ag^+ ion-conducting composite electrolyte system: $(1-x)$ (0.75AgI:0.25AgCl):xAl_2O_3 are reported. Undried Al_2O_3 particles of size < 10 μm were used. The conventional matrix material AgI has been replaced by a new mixed 0.75AgI:0.25AgCl quenched and/or annealed host compound. Conductivity enhancements ~ 10 from the annealed host and ~ 3 times from the quenched host obtained for the composition $0.7(0.75AgI:0.25AgCl):0.3Al_2O_3$, can be explained on the basis of the space charge interface mechanism. Direct measurements of ionic mobility μ as a function of temperature together with the conductivity σ were carried out for the best composition. Subsequently, the mobile ion concentration n values were calculated from μ and σ data. The value of heat of ion transport q^* obtained from the plot of thermoelectric power θ versus $1/T$ supports Rice and Roth's free ion theory for superionic conductors. Using the best composition as an electrolyte various solid state batteries were fabricated and studied at room temperature with different cathode preparations and load conditions.

1. Introduction

Heterogeneous composite electrolytes are a new class of high ionically conducting materials which have attracted considerable attention in recent years due to their potential technological applications. These materials are multiphase, mostly two phase, systems where a significant conductivity enhancement is achieved simply by the dispersion of ultrafine (submicron size) particles of inert and insoluble second phase (such as Al_2O_3, SiO_2, Fe_2O_3, fly-ash etc.) into the first phase host matrix (such as AgI, AgBr, AgCl, LiI, CuCl, CaF_2 etc.) [1–9]. Though the conductivity enhancement in the two phase system was known for about 75 years [10], the systematic investigations started only after 1973 when C. C. Liang reported ~ 50 times enhancement of Li^+ ion conduction in the $LiI:Al_2O_3$ dispersed system [11]. Since then a large number of two phase composite electrolyte systems with Ag^+, Li^+, Cu^+, F^- etc. ion conduction have been reported with conductivity one to three orders of magnitude higher than the constituent phases. Many phenomenological models have been proposed to explain the conductivity enhancement in these electrolyte systems [1–6, 12–16]. The central feature of the majority of these models is the increase in the mobile ion concentration at the interfacial space charge region of the host matrix/dispersoid. Moreover, a well-connectivity of these interfacial regions creating highly conducting paths would be necessary to facilitate high ionic motion. The volume fraction and the particle size of the second phase dispersoid play crucial roles in the conductivity enhancement. In addition to this, the dispersion of the submicron size particles of the inert second phase may also change the chemistry and microstructure of the host matrix which might control the transport mechanism in these systems. The conductivity enhancements in different composite systems (made of different matrix materials, different compositions, following different preparation routes etc.) cannot be understood by any single mechanism [5]. Hence, the present day goal is to search for a unified model explaining the greatly enhanced carrier concentrations or mobilities in these systems.

In the present paper, we report the preparation of a new fast Ag^+ ion conducting composite electrolyte system: $(1-x)(0.75AgI:0.25AgCl):xAl_2O_3$, where the conventional host matrix AgI is replaced by a new host, a quenched and/or annealed 0.75AgI:0.25AgCl mixed system. The detailed investigations related to the new host material appear elsewhere in the literature [17]. The electrical conductivity σ of the composites were measured as a function of molar concentration x, routes of preparation, temperature etc. whereas the direct measurement of ionic mobility

* Author to whom correspondence should be addressed.

0022–2461

μ and thermoelectric power θ at various temperatures were performed only on the best composition. Subsequently, the mobile ion concentration n and heat of ion transport were evaluated. Using the best composition as an electrolyte, solid state batteries were fabricated and the discharge characteristics were studied at different load conditions and with various cathode preparations.

2. Experimental procedure

2.1. Sample preparation

Extra pure chemicals AgI, AgCl and Al_2O_3 (particle size <10 μm) were used as supplied. Composite electrolyte systems $(1-x)$ $(0.75AgI:0.25AgCl):xAl_2O_3$, where x is mol wt %, were synthesized following different preparatory routes as given below:

1. (Quenched/Annealed host + Al_2O_3) → heated at ~700 °C for 15 min (soaking time) then quenched at ~10 °C;
2. (Quenched host + Al_2O_3) → physical mixture;
3. (Annealed host + Al_2O_3) → heated at ~700 °C then annealed at ~200 °C for 24 h;
4. (Annealed host + Al_2O_3) → physical mixture annealed at ~200 °C for 24 h.

Further, composite electrolyte systems $(1-x)$ $AgI:xAl_2O_3$ were also prepared following route (1) using the conventional host AgI for direct comparison of the room temperature conductivity values with that of the new composite systems.

The samples were ground to fine powder then pressed at ~1.5 t to form pellets of dimensions 2–3 mm in thickness and ~1.185 cm in diameter. Colloidal silver paint was used as electrodes for conductivity measurements.

2.2. Transport property measurements

The electrical conductivity was measured as a function of temperature by an impedance spectroscopic technique in the frequency range 40 Hz–100 kHz. The true bulk conductivity was computed from Z'–Z'' impedance plot with the help of a computer controlled LCR bridge (Hioki, Model 3520-01).

The ionic mobility as a function of temperature and transference number were measured for the best composition only using the transient ionic current technique [18–21] and Wagner's d.c. polarization method respectively. A Graphtec x–y–t recorder (model WX 2300-1L) was used in both the measurements.

The thermoelectric power (TEP) θ measurements at different temperatures were carried out for the best composition with the help of digital multimeters (Philips model 2518). The sample pellet was placed between two Ag–metal electrodes. The ambient temperature was controlled by an external heater and a temperature gradient ΔT ~10–15 °C between the two faces of the pellet across the thickness was maintained by an auxiliary heater fitted to the upper electrode of the sample holder. Sufficient intervals (~2–3 h) were given for recording each stabilized thermo-e.m.f. values.

2.3. Solid state battery fabrication

Solid state batteries were fabricated using the best composition as an electrolyte in the following cell configuration

$$\text{Anode} \,/\, \begin{matrix} Ag^+ \text{ ion conducting} \\ \text{composite electrolyte} \end{matrix} \,/\, \text{Cathode}$$

Silver metal was used as anode whereas different cathode preparations such as $C + I_2$, $C + KI_3$, $C + (CH_3)_4NI_3$, $C + (C_2H_5)_4NI_3$, etc. in 1:1 wt ratio were used as cathodes for the discharge characteristic studies at different load conditions. Chelated iodines were prepared by heating the mixture of $KI + I_2$, $(CH_3)_4NI + I_2$ and $(C_2H_5)_4NI + I_2$ in a 1:1 mol wt ratio in separate sealed silica tubes at ~150 °C for 24 h. A Philips digital multimeter was employed for cell potential measurements. The batteries were sealed with epoxy resin to inhibit the surface diffusion of iodine. All the measurements were performed in a desiccator to avoid the effect of moisture.

3. Results and discussion

3.1. Compositional variation of room temperature conductivity: influence of preparation routes and soaking time

Fig. 1 shows the variation of room temperature conductivity of $(1-x)$ $(0.75AgI:0.25AgCl):xAl_2O_3$ composite systems as a function of mol wt ratio x following various preparation routes (1–4), as mentioned in Section 2.1. Similar variation (curve 5), for the composite system: $(1-x)AgI:xAl_2O_3$, prepared following route (1), is also included in Fig. 1 for direct comparison. One can note a much larger conductivity enhancement in the composite system using the new host as compared to that using AgI as host, even with the dispersion of much bigger particles (size <10 μm) of second phase Al_2O_3. One may expect more enhancement in the conductivity for the new composite system if the particle size is further reduced. Shahi and Wagner [8] reported very little conductivity enhancement in the $(1-x)AgI:xAl_2O_3$ composite system using Al_2O_3 particles of size ~8 μm. Their and the present results are qualitatively similar. However, they

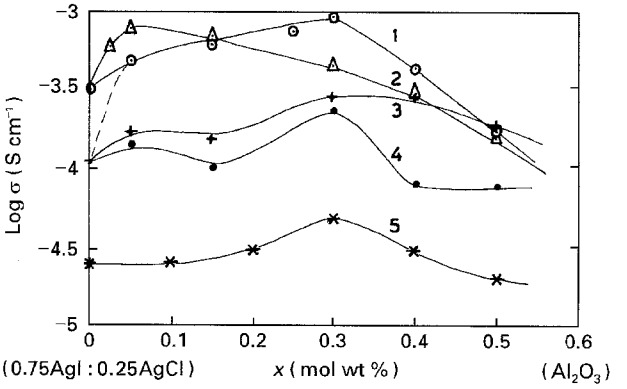

Figure 1 Log σ versus x plots for composite systems $(1-x)$ $(0.75AgI:0.25AgCl):xAl_2O_3$, prepared by following different routes: Curves (1–4) correspond to preparation routes (1–4) (See text section 2.1); Curve (5) is similar plot for the composite system $(1-x)$ $AgI:xAl_2O_3$, prepared following route (1). All at 27 °C.

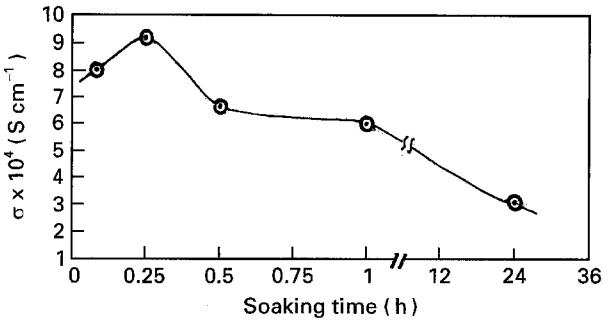

Figure 2 Room temperature conductivity as a function of soaking time for the best composition, $0.7(0.75AgI:0.25AgCl):0.3Al_2O_3$ (prepared by route 1). Soaking temperature $\simeq$ 700 °C.

differ quantitatively due to the different purities of starting materials used in our studies. The maxima in the conductivity vary with the preparation routes. However, the conductivity increases effectively in all cases with the increase in x, attains a peak value, then decreases. This is a well-known phenomenon generally observed in composite systems and can be explained in the light of percolation approach [13]. We obtained, the highest conductivity enhancement, ~ 10 and ~ 3 times from the annealed and quenched host 0.75AgI:0.25AgCl respectively, for the composition $0.7(0.75AgI:0.25AgCl):0.3Al_2O_3$ prepared following route (1) with soaking time $\simeq$ 15 min.

Soaking time, for which the sample is heated at $\sim$700 °C during the preparation, affects the physical property of the composite system. To examine the influence of soaking time on the conductivity, samples of the best composition: $0.7(0.75AgI:0.25AgCl):0.3Al_2O_3$ were prepared following route (1) but for different soaking times. Fig. 2 gives the variation of room temperature conductivity with soaking times. It is clear from the figure that the highest conductivity value resulted for the 15 min soaking time. The decreased values of conductivity for lower and higher soaking times are probably due to the incomplete dispersion reaction and change in the stoichiometry due to possible liberation of iodine, respectively.

3.2. Ionic transference number and temperature dependence of σ, μ and n

Ionic transference number (t_{ion}) was measured for the best composition only using Wagner's d.c. polarization method as mentioned in Section 2.2. A d.c. potential ($V \sim 0.5$ V), with the polarity shown below was applied across the sample pellet in the following configuration

$$\begin{array}{c|c|c} (-)\text{Ag} & & \text{C}(+) \\ \text{(non-blocking} & 0.7(0.75\ \text{AgI}:0.25\ \text{AgCl}): & \text{(blocking} \\ \text{electrode)} & 0.3\ Al_2O_3 & \text{electrode)} \end{array}$$

The total current was monitored with time. From the current versus time plot, we obtained $t_{ion} \sim 1$. This indicates that the Ag^+ ions are the sole charge carriers in this system. This result is also confirmed by an alternate method discussed below in Section 3.4.

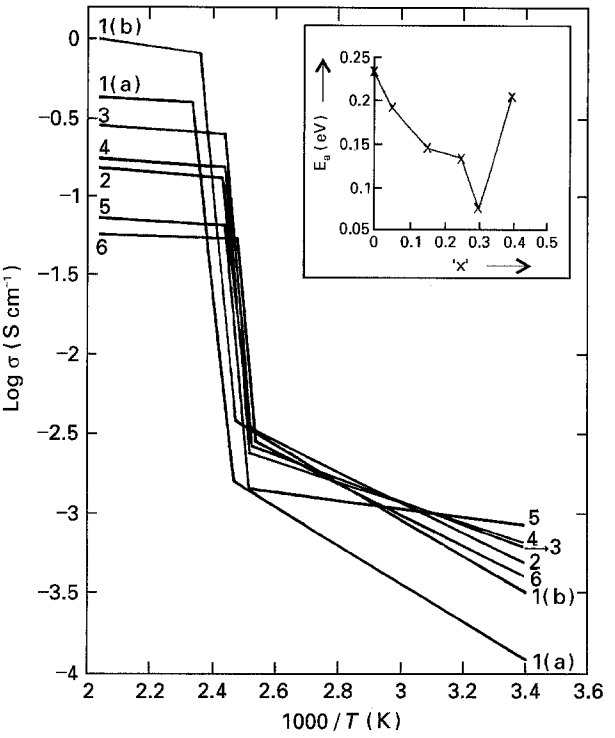

Figure 3 Log σ versus $1/T$ plot for composite system $(1-x)(0.75AgI:0.25AgCl):xAl_2O_3$ prepared by route (1). (a) $x = 0$ (pure annealed host); (b) $x = 0$ (pure quenched host); (2) $x = 0.05$; (3) $x = 0.15$; (4) $x = 0.25$; (5) $x = 0.30$; (6) $x = 0.40$. Inset: Activation energy (E_a) as a function of x for the above compositions in the temperature range 27–120 °C.

Fig. 3 shows log σ versus $1/T$ plots for the different compositions of the composite system: $(1-x)(0.75AgI:0.25AgCl):xAl_2O_3$ prepared following route (1) where $x = 0.05$, 0.15, 0.25, 0.30 and 0.40 (curves 2–6). Similar plots [curves 1(a) and (b)] for annealed and quenched host system (0.75AgI: 0.25AgCl) are also shown in Fig. 3. The room temperature conductivity increases up to $x = 0.3$ then decreases for higher concentrations, as discussed above in section 3.1. The conductivity enhancements may be attributed to the increased mobile ion concentration and/or mobility at the interfacial space charge region. The enhancement by dispersion of Al_2O_3 particles is accompanied by decrease in activation energy, as is usual for most high ionically conducting systems. This is also true for the above composite systems. The activation energy values, computed from the slopes of log σ versus $1/T$ plots, for the annealed host, the quenched host and the composite systems are given in Table I together with the room temperature conductivity values and pre-exponential factors. The E_a versus x variation is shown as an inset in Fig. 3. The activation energy for the best conductivity composition is very small ($\sim$ 0.074 eV) which indicates an easy ion migration in this system.

The Ag^+ ion mobility as a function of temperature was calculated using the transient ionic current (TIC) technique, as mentioned in Section 2.2. In this technique a d.c. potential $V \sim 0.5$ V is applied across the sample which is sandwiched between two blocking (graphite) electrodes. The cell is first polarized completely, then the polarity is reversed and the current is

TABLE I Various transport parameters for the composite electrolyte system $(1-x)$ (0.75 AgI: 0.25 AgCl): xAl_2O_3, prepared by route (1) together with annealed and quenched host

x m/o	Conductivity σ ($s\,cm^{-1}$) at 27 °C	Ionic mobility μ ($cm^2\,V^{-1}\,s^{-1}$) at 27 °C	Mobile ion concentration n (cm^{-3}) at 27 °C	Pre-exp factor σ_0	Activation energy E_a (eV)	Temperature range (°C)
0.00	1.26×10^{-4} (Annealed)	$(1.5\pm1)\times10^{-2}$	4×10^{16}	1.78	0.243	27–120
	3.14×10^{-4} (Quenched)	$(2.4\pm1)\times10^{-2}$	8×10^{16}	3.22	0.234	27–120
0.05	4.80×10^{-4}	–	–	1.01	0.194	27–120
0.15	6.10×10^{-4}	–	–	0.19	0.145	27–120
0.25	7.06×10^{-4}	–	–	0.12	0.133	27–120
0.30	9.20×10^{-4}	$(2.4\pm1)\times10^{-2}$	2.4×10^{17}	0.016	0.074	27–120
0.40	4.30×10^{-4}	–	–	1.191	0.203	27–120

recorded with time. The moment the polarized ion cloud reaches the other end of the sample, a peak occurs in the current versus time plot. This peak corresponds to the time τ taken by the ions to cross the thickness d of the sample. The ionic mobility can be calculated by following equation

$$\mu = d^2/V\tau\,(cm^2\,V^{-1}\,s^{-1}) \quad (1)$$

Using the conductivity (σ) and mobility (μ) data, the mobile ion concentration (n) at different temperatures can be calculated by the well-known expression

$$n = \sigma/q\,\mu\,(cm^{-3}) \quad (2)$$

The room temperature values of μ and n for the annealed host, the quenched host and the best composition are given in Table I. The μ values practically remained unaltered whereas n increases ~3–6 fold from that of the quenched–annealed hosts, respectively. These results clearly indicate that the reason for the conductivity enhancement in the composite system at room temperature is the increase in mobile ion concentration.

Fig. 4 shows plots of $\log\mu$ versus $1/T$ and $\log n$ versus $1/T$ for the best composition. The mobility μ increases as the temperature is increased to ~100 °C (Region I), then decreases sharply (Region II). Whereas there is a little decrease in the mobile ion concentration n at the beginning, it then increases abruptly after ~100 °C. The increase in μ with temperature is a well-known phenomenon, but the reason for small decrease in n is not clear. However, this decrease in n is well-compensated for by the increase in μ and the overall conductivity increases. We obtained almost identical μ and n variations with the temperature for the quenched host [17]. The onsets of the changes in the Region I well ahead of the transition region may be attributed to pretransition effects. The decrease in the mobility (in Region II) is attributed to the structural volume contraction of the host compound resulting into space narrowing for ion migration as well as to the blocking effect of Al_2O_3 particles. The abrupt increase in n (in Region II) is due to the fact that the host acquires an entirely new

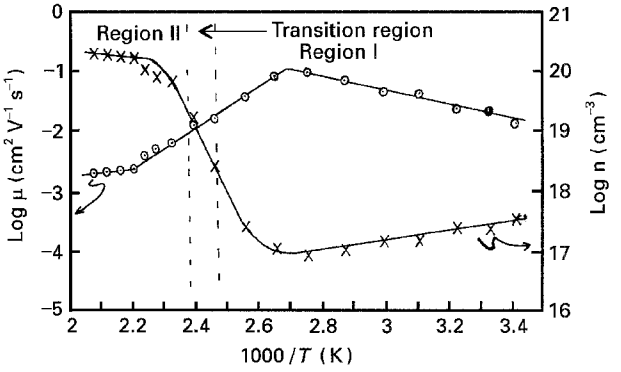

Figure 4 Log μ versus $1/T$ ($\odot$) and Log n versus $1/T$ (x) plots for the best composition: 0.7 (0.75AgI:0.25AgCl):0.3Al_2O_3.

structure (α-like phase of AgI) where a large number of equienergetic Ag^+ ions become available for conduction. Table II gives the Arrhenius equations governing the temperature variation of σ (curve 5 of Fig. 3), μ and n along with the values of pre-exponential factors, conductivity activation energy (E_a), energy of migration (E_m) and energy of formation (E_f). These energy values satisfy very well the following equation in the two Regions (I and II) [21–23]

$$E_a = \pm E_m \pm E_f \quad (3)$$

The (+) and (−) signs in the Arrhenius equations of Table II indicate the decrease and increase, respectively, of the quantities (σ, μ and n) with the increase in temperature.

3.3. Thermoelectric power (TEP) measurements

Thermoelectric power (TEP) studies provide further insight into understanding the ion transport mechanism in these high ionically conducting systems. When a temperature gradient (ΔT) exists across the sample in the following cell configuration:

$$Ag\,(T)\,\Big/\,\begin{matrix}Ag^+\text{ ion conducting}\\ \text{solid electrolyte}\end{matrix}\,\Big/\,Ag\,(T+\Delta T)$$

TABLE II Pre-exponential factors, conductivity activation energy (E_a), energy of migration (E_m) and energy of formation (E_f) for the best composition: 0.7 (0.75 AgI: 0.25 AgCl): 0.3 Al_2O_3 (preparation route 1)

Region	$\sigma = \sigma_0 \exp(-E_a/kT)$		$\mu = \mu_0 \exp(\mp E_m/kT)$		$n = n_0 \exp(\mp E_f/kT)$		Temp. range (°C)
	σ_0	E_a (eV)	μ_0	E_m (eV)	n_0	E_f (eV)	
I	0.016	0.074	100.5	0.219	9.8×10^{14}	− 0.145	27–100
II	0.135	0.024	9.3×10^{-5}	− 0.129	9.4×10^{21}	0.154	180–215

a voltage (ΔV) appears across the two faces of the sample due to the Ag^+ ions' flow from the hot to the cold end. The TEP θ can be calculated by following equation [24]

$$\theta = \Delta V/\Delta T \quad (4)$$

Theoretically, the thermoelectric power has been calculated as [25]

$$-\theta = (q^*_{Ag^+}/eT) - H \quad (5)$$

where q^* is the heat of Ag^+ ion transport, e is the charge on the mobile ion and H is a correction term for the electrode contact potential effects. For the reversible electrodes, such as the silver metal electrodes in the above thermocell, H is constant. Hence, a plot of θ versus $1/T$ would be a straight line and the value of the heat of ion transport q^* in eV can be calculated from the slope of the line.

Fig. 5 shows the variation of TEP θ with the reciprocal of temperature in (K) for the best composition. θ decreases with the increasing temperature in Region I, followed by a drop in the transition region then remains practically unchanged in Region II. The decrease in θ with temperature is a typical behaviour exhibited by fast ion-conducting solids and is in accordance with theory [25]. The heats of ion transport equal to ~0.07 and ~0.02 eV calculated from the slopes of the straight lines in Region I and Region II respectively, are in excellent agreement with the conductivity activation energy values: 0.074 and 0.024 eV listed in Table II. These results receive direct support from Rice and Roth's free ion theory [26] for superionic solids, according to which the heat of ion transport is very close to the conductivity activation energy for solids possessing an average structure and free-ion like state.

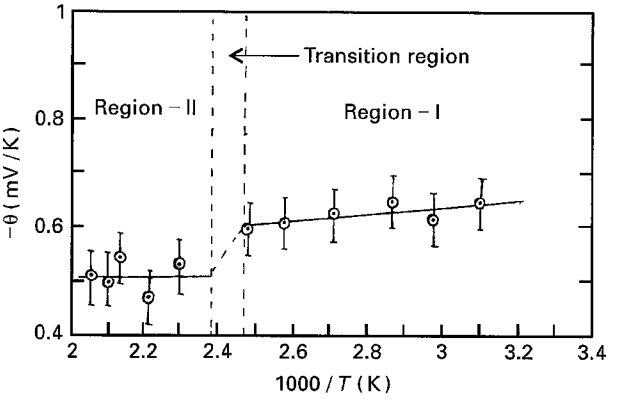

Figure 5 Thermoelectric power (TEP) θ versus $1/T$ plot for the best composition: 0.7 (0.75AgI: 0.25AgCl): 0.3Al_2O_3.

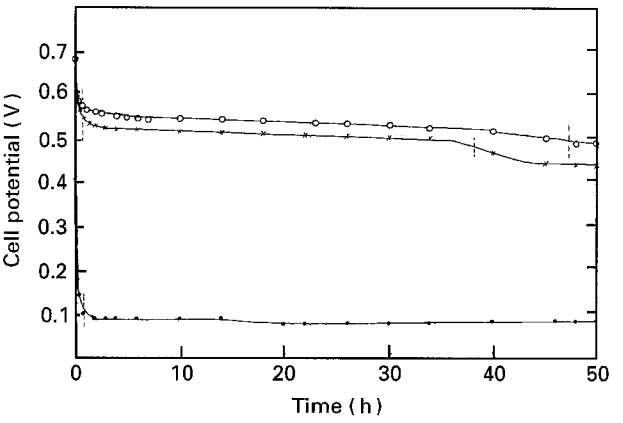

Figure 6 Variation of cell potential with time through different loads for solid state batteries in the configuration Ag [Anode]/Ag^+ ion conducting composite/(C + I_2) [Cathode]. Dotted vertical bars indicate the plateau region. ○ 1 MΩ; × 226 kΩ; ● 22 kΩ.

3.4. Solid state battery applications and transference number by cell potential method

Fig. 6 shows the variations of cell potential with time at different load conditions, namely 1 MΩ, 226 kΩ, 22 kΩ for the solid state batteries fabricated with the best composition in the cell configuration mentioned in Section 2.3. using (C + I_2) cathode. The open circuit voltage (OCV) ~0.685 V was obtained for all the batteries. The cell potential remained practically constant (~ 0.550–0.525 V), except for an initial drop from the OCV values for over 50 h with 1 MΩ and 226 kΩ loads, whereas it dropped to ~ 0.090 V within a short time (~30 min) for a 22-kΩ load. The drop in the cell potential is due to the build up of polarization and the formation of low conducting AgI at the electrolyte/cathode interface which are very fast in the case of low loads or at high current drains.

To examine the influence of different cathodes on the cell performance, we fabricated several batteries in the same cell configuration using different cathode preparations, namely KI_3 + C, $(CH_3)_4NI_3$ + C, $(C_2H_5)_4NI_3$ + C as mentioned in Section 2.3. Fig. 7 gives the variation of cell potential with time through 1 MΩ load. The discharge curve of Fig. 6 for a 1-MΩ load is redrawn in Fig. 7 for direct comparison. It is normally expected that the use of a chelated iodine cathode improves the performance and shelf-life of the battery, since chelation reduces the activity and tarnishing action of the elemental iodine towards the

electrolyte and metal electrodes [27, 28]. However, the batteries using chelated iodine cathodes discharged more rapidly as compared to those with elemental iodine as cathode. It is obvious from these experimental results that batteries fabricated with (C + I_2) cathodes have better performance specially with low drain load currents. Some of the typical cell parameters calculated in the plateau region of the discharge characteristic curves of Fig. 6 are listed in Table III.

The ionic transference number (t_{ion}), determined earlier in Section 3.2 using Wagner's d.c. polarization method, can also be evaluated by electrochemical cell potential method using following equation [27, 29]

$$t_{ion} = \frac{E'}{E} \tag{6}$$

where E' and E are the measured and theoretical values of OCV respectively. We obtained $E' \sim 0.685$ V, whereas the theoretical value of OCV, involved in the cell reaction $Ag^+ + I^- = AgI$ at the electrolyte/cathode interface with elemental iodine as cathode, $E \sim 0.687$ V [27]. We obtained $t_{ion} \sim 0.997$ which is extremely close to the value obtained earlier.

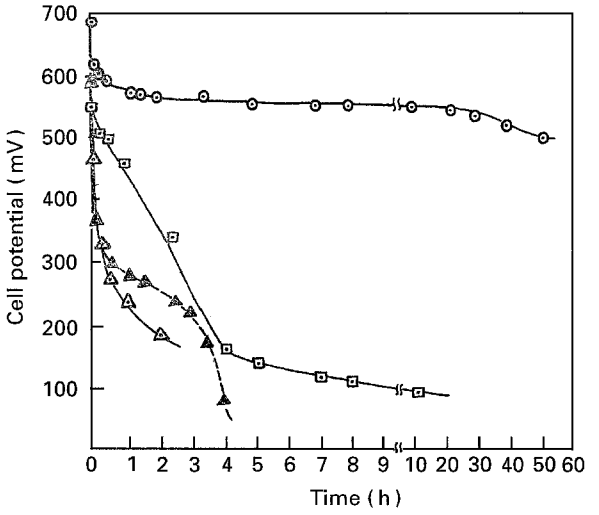

Figure 7 Variation of cell potential with time for the solid state batteries in the above cell configuration with different cathode preparations. Load 1 MΩ; ⊙ Ag/0.7(0.75AgI:0.25AgCl) $0.3Al_2O_3/(I_2 + C)$ OCV ~ 685 mV; ▲ Ag/0.7(0.75AgI:0.25AgCl) $0.3Al_2O_3/(KI_3 + C)$ OCV ~ 590 mV; ⊡ Ag/0.7(0.75AgI: 0.25AgCl) $0.3Al_2O_3/(CH_3)_4NI_3 + C$ OCV ~ 550 mV; △ Ag/0.7(0.75AgI:0.25AgCl) $0.3Al_2O_3/(C_2H_5)_4NI_3 + C$ OCV ~ 590 mV.

4. Conclusion

A new fast Ag^+ ion-conducting composite electrolyte system $0.7(0.75AgI:0.25AgCl):0.3Al_2O_3$ has been investigated. The conventional host compound AgI is replaced by a new matrix material, a quenched and/or annealed 0.75AgI:0.25AgCl mixed system. Conductivity enhancement (~10) from the annealed host was achieved at room temperature even by dispersing a much larger size (< 10 μm) of Al_2O_3 particles. The enhancement in the conductivity is attributed to the increased mobile ion concentration at the matrix/dispersoid interface region. Detailed studies on preparation methods, transport properties and solid state battery applications are reported. The batteries fabricated with a C + I_2 cathode give better performance and are suitable for low current drain applications.

Acknowledgement

We would like to thank the University Grant Commission (UGC) for the financial support through major research project no. F-10-4/90(SR-I) dt.11.07.91.

References

1. J. MAIER, in "Solid state ionics: materials and applications", edited by B. V. R. Chowdari, S. Chandra, S. Singh and P. C. Srivastava (World Scientific, Singapore, 1992) p. 111.
2. A. K. SHUKLA and V. SHARMA, *ibid.* p. 91.
3. J. MAIER, in "Superionic solids and solid electrolytes – recent trends", edited by A. L. Laskar and S. Chandra (Academic Press, New York, 1989) p. 137.
4. J. B. WAGNER, in "High conductivity solid ionic conductors – recent trends and applications", edited by T. Takahashi (World Scientific, Singapore, 1989) p. 146.
5. N. J. DUDNEY, *Ann. Rev. Mater. Sci.* **19** (1989) 103.
6. F. W. POULSEN, in "Transport–structure relations in fast ion and mixed conductors" edited by F. W. Poulsen, N. H. Andersen, K. Clausen, S. Skaarup and O. T. Sorensen (Riso Nat. Lab., Roskilde, Denmark, 1985) p. 67.
7. T. JOW and J. B. WAGNER, Jr, *J. Electrochem. Soc.* **126** (1979) 1963.
8. K. SHAHI and J. B. WAGNER, Jr, *ibid.* **128** (1981) 6.
9. C. C. LIANG, A. V. JOSHI and N. E. HAMILTON, *J. Appl. Electrochem.* **8** (1978) 445.
10. W. JANDER, *Angew. Chem.* **42** (1929) 462.
11. C. C. LIANG, *J. Electrochem. Soc.* **120** (1973) 1289.
12. M. F. BELL, M. SAYER, D. S. SMITH and P. S. NICHOLSON, *Solid State Ionics* **9/10** (1983) 731.
13. A. BUNDE, W. DIETERICH and E. ROMAN, *Phys. Rev. Lett.* **55** (1985) 5.
14. R. BLENDER and W. DIETERICH, *J. Phys. C.* **20** (1987) 6113.
15. N. F. UVAROV, V. P. ISUPOV, V. SHARMA and A. K. SHUKLA, *Solid State Ionics* **51** (1992) 41.
16. U. LAUER and J. MAIER, *Ber. Bunsenges. Phys. Chem.* **96** (1992) 111.

TABLE III Typical cell parameters calculated in the plateau region of the discharge curves of the solid state battery Ag/Ag^+ ion conducting composite/(C + I_2)

Load kΩ	Cell size (mm^3)	Cell weight (g)	Working voltage in the plateau region (Vs)	Current density ($\mu A\,cm^{-2}$)	Discharge capacity (μA h)	Power density ($mW\,Kg^{-1}$)	Energy density ($mW\,h\,Kg^{-1}$)
1000	7×7×3	1.35	0.550	1.1	25.8	0.2	10.5
226	7×7×3	1.31	0.525	4.7	88.2	0.9	35.2
22	7×7×3	1.28	0.090	8.4	73.6	0.3	5.2

17. R. C. AGRAWAL, R. K. GUPTA, R. KUMAR and A. KUMAR, *J. Mater. Sci.* **29** (1994) 3673.
18. M. WATANABE, K. SANUI, N. OGATA, T. KOBAYASHI and Z. ONTAKI, *J. Appl. Phys.* **57** (1985) 123.
19. S. CHANDRA, S. K. TOLPADI and S. A. HASHMI, *Solid State Ionics* **28/30** (1988) 651.
20. R. C. AGRAWAL, K. KATHAL, R. CHANDOLA and R. K. GUPTA, in "Solid state ionics: materials and applications", edited by B. V. R. Chowdari, S. Chandra, S. Singh and P. C. Srivastava (World Scientific, Singapore, 1992) p. 363.
21. R. C. AGRAWAL, K. KATHAL and R. K. GUPTA, *Solid. State Ionics* **74** (1994) 137.
22. R. C. AGRAWAL and R. KUMAR, *J. Phys. D.* **27** (1994) 2431.
23. K. M. SHAJU and S. CHANDRA, *Phys. Stat. Sol.* (*b*) **181** (1994) 301.
24. K. SHAHI, *Phys. Stat. Sol.* (*a*) **41** (1977) 11.
25. S. M. GIRVIN, *J. Sol. Stat. Chem.* **25** (1978) 65.
26. M. J. RICE and W. L. ROTH, *ibid.* **4** (1972) 294.
27. S. CHANDRA and R. C. AGRAWAL, "Solid state battery – prospects and limitations" (National Academy of Sciences, India: Golden Jubilee Commemoration Volume, 1980) p. 1.
28. P. HAGENMULLER and W. van GOOL (editors), "Solid electrolytes", Material Science Series (Academic Press, 1978).
29. K. KIUKKOLA and C. WAGNER, *J. Electrochem. Soc.* **104** (1957) 308 & 379.

Received 27 April 1994
and accepted 3 February 1995